Fluctuations in marine radiocarbon reservoir age in the western Pacific: Evidence of reduced E–W Pacific gradient over the past 6000 years

Hong-Wei Chiang[1*], J. Bruce H. Shyu[1*], Sze-Chieh Liu[1], Chung-Che Wang[1], Chuan-Chou Shen[1,2,3,4], George S. Burr[1], Shing-Lin Wang[1], Yoko Ota[1]

[1]Department of Geosciences, National Taiwan University, Taipei 10617, Taiwan, ROC

[2]High-Precision Mass Spectrometry and Environment Change Laboratory (HISPEC), Department of Geosciences, National Taiwan University, Taipei 10617, Taiwan, ROC

[3]Research Center for Future Earth, National Taiwan University, Taipei 10617, Taiwan, ROC

[4]Global Change Research Center, National Taiwan University, Taipei 10617, Taiwan, ROC

***Corresponding authors:**

Hong-Wei Chiang, Department of Geosciences, National Taiwan University, Taipei 10617, Taiwan, ROC

E-mail: hwchiang@ntu.edu.tw

J. Bruce H. Shyu, Department of Geosciences, National Taiwan University, Taipei 10617, Taiwan, ROC

E-mail: JBHS@ntu.edu.tw

Abstract

Radiocarbon (^{14}C) is a useful tracer for surface ocean circulation and mixing, which reflects air-sea CO_2 exchange. We present radiocarbon marine reservoir ages (R) and corrections (ΔR) in Holocene inferred from 18 paired ^{14}C and ^{230}Th ages on fossil corals from Lanyu Island offshore eastern Taiwan. The results show large fluctuations in the ΔR value, with averages of -330 and -5 ^{14}C yr for 6000–5100 yr BP and the past 150 years, respectively. The extremely young R in the mid-Holocene indicate a well-equilibrated North Equatorial Current (NEC), likely stemmed from enhanced air-sea interactions and strengthened Pacific Walker circulation. This suggests a larger E–W gradient across the Equatorial Pacific and hence a La Niña-like condition, consistent with both model simulations and other paleo-proxy records. Combining the ΔR records in the northern South China Sea, the results imply an increasing influence of the NEC water on the subtropical western Pacific since the mid-Holocene.

Keywords

Corals; U–Th dating; Radiocarbon dating; Marine reservoir age (R); Marine reservoir correction (ΔR); Pacific walker circulation

Plain Language Summary

The heat gradient across the Pacific Ocean induces the zonal winds, which were once important to the voyage and navigation in human history, and also plays a critical role on modulating global climate. However, its evolution through time is less known. Here we use radiocarbon in corals from the western Pacific as an archive of air-sea interaction which is influenced by wind speed, and in terms the heat gradient. The results show large variations in radiocarbon content over diverse timescales. This suggests a period of strong gradient 6000-5000 years ago and is consistent with other studies. The past 1000 years was inferred to have relatively weaker zonal winds, which could have been caused by more frequent occurrence of El Niño-Southern Oscillation events.

Key Points:

1. This study is the first to report temporally fluctuated R/ΔR in the western Pacific during the Holocene by paired coral ^{14}C and ^{230}Th ages.
2. The greatly reduced ΔR values in 6000-5000 yr BP imply a well-ventilated seawater and possibly a larger E–W gradient across the Pacific.
3. The identical ΔR from Lanyu and northern South China Sea in late Holocene suggests a dominant influence of the North Equatorial Current.

1. Introduction

The Pacific Walker Circulation (PWC) is an east–west overturning atmospheric circulation in the equatorial region that ascends in the west and descends in the east. It plays an important role in modulating global climate, because strong atmosphere-ocean interactions and heat transfer take place within this belt. In modern times, its interannual to decadal variabilities are closely linked to El Niño-Southern Oscillation (ENSO) and Pacific Decadal Oscillation (PDO) (Hu et al. 2015; Kashino et al., 2009; Qiu, 2003). However, the dynamics of ENSO on longer timescales is still open to debate. Modeling and palaeoclimate studies showed that El Niño frequency and amplitude reduced in the early to mid-Holocene (McGregor and Gagan, 2004; McGregor et al., 2008; Moy et al., 2002; Tudhope et al., 2001), whereas some studies (Zhang et al., 2014) suggested that frequent ENSO events occurred at that time, or that there was no systematic trend in ENSO frequency or strength in the Holocene (Cobb et al., 2013). Thus, understanding PWC variation not only affords an opportunity to resolve these conflicting views on ENSO, but is also important for climate projection.

Radiocarbon (^{14}C) is a useful tracer for seawater mass mixing (Broecker 2014; Burr et al., 2015; Druffel, 1997; Druffel & Griffin, 1999; Grottoli & Eakin, 2007; Hua et al., 2015; Ramos et al., 2019; Southon et al., 2002), which is always affected or accompanied by climatic events. The basic idea is that deep waters are ^{14}C-depleted, while surface waters are relatively ^{14}C-enriched. The ^{14}C content of a regional water mass is distinctive, and generally depends on horizontal advection and vertical mixing processes. Changes of regional seawater ^{14}C consequently indicate a change in oceanography or hydrology. In addition, the ^{14}C content of a water mass can be used to determine an “age”, relative to the contemporaneous atmosphere. This is termed

100 the radiocarbon marine reservoir age (R). A location-specific R value can also be
101 expressed as ΔR, the deviation from a global mean ocean reservoir age based on a
102 model ocean that responds to known changes in atmospheric ^{14}C (Stuiver et al., 1986).
103 In general, higher R or ΔR values indicate more ^{14}C depletion.

104 Coral skeletons have been widely used as high-resolution paleoclimate archives
105 that have two significant advantages: (1) they can be precisely dated by both ^{14}C and
106 ^{230}Th methods, and (2) they are widely distributed in the world oceans. Corals draw
107 on dissolved inorganic carbon (DIC) in seawater for calcification, and radiocarbon
108 values in their skeletons closely reflect seawater DIC ^{14}C values, independent of
109 metabolic fractionation (Moyer & Grottoli, 2011; Nozaki et al., 1978). Therefore,
110 corals are a good archive to study the radiocarbon variations caused by deep-water
111 upwelling, air-sea interactions, and terrigenous discharges. Several previous coral
112 studies have combined radiocarbon and ^{230}Th dates to determine pre-bomb ΔR values
113 in eastern Taiwan and the Ryukyu Islands (Araoka et al., 2010; Hirabayashi et al.,
114 2017a).

115 Here we have reconstructed marine reservoir ages (R) and corrections (ΔR)
116 over the past 6,000 years from Lanyu Island, a small island off the east coast of
117 Taiwan, using paired ^{14}C and U–Th dates from 18 fossil corals. The results show a
118 remarkable variability in ΔR and challenge the assumption of constant ΔR through the
119 mid- to late Holocene. We also compared our results with reported values from the
120 northern South China Sea. The results suggest a changing air-sea interaction in the
121 NEC, which is linked to easterly winds in the tropics and the Pacific Ocean
122 conditions.

123

124 **2. Study sites and materials**

125 The main stream of the Kuroshio Current (KC) flows northward along the east
126 coast of Taiwan with a transport rate of 15–47 Sv (1 Sv = 10^6 m^3s^{-1}) depending on the
127 season (Hsin et al., 2008; Lee et al., 2001; Liang et al., 2003). At minimum KC
128 strength in winter, the North Equatorial Current (NEC) bifurcation shifts northward
129 (Qu & Lukas, 2003), and the flow of NEC water into the northern SCS through the
130 Luzon Strait increases (Yaremchuk & Qu, 2004) (Fig. 1a). The situation in summer is
131 reversed when the southwest monsoon prevails. On multi-year timescales, a strong El
132 Niño condition corresponds to a weaker PWC, a northward shift of the NEC
133 bifurcation and a weaker KC (Masumoto & Yamagata, 1991; Tozuka et al., 2002).
134 Kuroshio water then crosses the 121°E line and reaches the northern SCS, similar to
135 winter conditions. Consequently, the KC is intensified and the penetration of KC into
136 the northern SCS is reduced during stronger PWCs, such as La Niña and cold PDO
137 phases.

138 Lanyu Island is situated at the northern end of the Luzon volcanic arc and is
139 fringed by 2–3 levels of Holocene coral reef terraces (Inoue et al., 2011; Ota et al.,
140 2015) (Fig. 1b). The area of Lanyu Island is ~50 square kilometers and has a
141 population of only ~3000. There are no major rivers but a number of local creeks.
142 Along the northern coast of Lanyu Island, nine large coral boulders were found at six
143 sites on the lowest Holocene terrace (Ota et al., 2015) (Fig. 1b). Eighteen fossil
144 *Porites* sp. corals (Fig. 1b) with less than 3% calcite content were selected for paired
145 ^{14}C and U–Th age determinations. Considering the potential seasonal variations in R
146 and ΔR, we combined coral fragments from a few growth bands (3–5 years).

147 The ^{14}C measurements were done by Beta Analytic, Inc. (Miami, FL), USA.
148 Five replicate measurements were also analyzed at the Xi'an Accelerator Mass
149 Spectrometry Center (XAAMS). For the U–Th dating, after crushing the coral

150 samples into segments, we then carefully picked out the most well-preserved pieces
151 under magnification, and ultrasonically cleaned with ultrapure water. Procedures of
152 U and Th chemical separation and purification are similar to those described by
153 Edwards et al. (1987) and Shen et al. (2003). The U and Th isotopic measurements
154 were performed on a Thermo Finnigan *NEPTUNE* MC-ICP-MS instrument in the
155 High-Precision Mass Spectrometry and Environmental Change Laboratory (HISPEC),
156 National Taiwan University. The determinations of ^{230}Th ages followed the methods
157 described by Shen et al. (2012).
158
159 **3. Results**
160 The R and ΔR values for the pre-1950 Common Era (CE) coral samples were
161 calculated as follows:
162 $$\Delta R(t) = Measured\ ^{14}C\ age - Marine\ model\ ^{14}C\ age(t) \quad (1),$$
163 $$R(t) = Measured\ ^{14}C\ age - Atmospheric\ ^{14}C\ age(t) \quad (2),$$
164 where ***t*** denotes the ^{230}Th age of coral in yr BP, and marine model and atmospheric
165 ^{14}C ages are based on the Marine09 and IntCal09 curves, respectively (Reimer et al.,
166 2009). In this study, U–Th dating provides the independent age estimates necessary
167 to determine past R and ΔR values. All errors of isotopic data and dates are given
168 with two standard deviation (2σ) uncertainties, unless otherwise noted.
169 Δ^{14}C values are also reported, which represent age- and δ^{13}C-corrected
170 proportional differences from the radiocarbon content of a sample, compared to the
171 1950 atmosphere. The ΔR (R) values can be inferred from the Δ^{14}C offset between
172 Marine09 (IntCal09) curve and corals, which retained the Δ^{14}C signal of local
173 seawater. The coral Δ^{14}C can be estimated by coupled calendar age and conventional
174 radiocarbon age of each sample [after *Stuiver and Polach*, 1977]:

$$\Delta^{14}C\ (‰) = \left(\frac{e^{\lambda_1 \times t_1}}{e^{\lambda_2 \times t_2}} - 1\right) \times\ 1000\ (‰) \quad (3),$$

where λ_1 is the decay constant based on the updated ^{14}C half-life of 5730 years; t_1 is the calendar age (U-Th age in this study); λ_2 is the decay constant based on Libby's half-life of 5568 years; t_2 is the reservoir (R)-corrected conventional radiocarbon age (without ΔR correction in Beta Analytic Inc.'s analyses). A larger ΔR value indicates a relatively older conventional marine ^{14}C age and hence smaller Δ^{14}C value, and vice versa.

All $\delta^{234}U_{initial}$ values are within the range of pristine coral aragonite (Stein et al., 1993; Stirling et al., 1995). The ^{14}C and ^{230}Th age results, and calculated R and ΔR values are presented in Table 1. The R and ΔR results show large fluctuations from 0 to 431 ^{14}C yr and -343 to 47 ^{14}C yr, respectively. On millennial timescales, ΔR increased from about -300 ^{14}C yr at 5–6 ka (n = 6) to near 0 ^{14}C yr for the most recent 150 years (n = 4), while R ranged from 35 ^{14}C yr in the mid-Holocene to 370 ^{14}C yr in the most recent 150 years. Meanwhile, the skeletal Δ^{14}C value moved from closer to the IntCal09 curve to within the realm of the Marine09 curve (Fig. 2).

The increase of ΔR and R values since the mid-Holocene is likely not due to hard-water effect since the fringing reefs on Lanyu Island were developed on igneous rock basements. Superimposed on the long-term trend are multi-year fluctuations. For instance, ΔR changed from 18 ± 38 ^{14}C yr at 152 cal yr BP, and 47 ± 38 ^{14}C yr at 144 cal yr BP, to -80 ± 38 ^{14}C yr at 142 cal yr BP. The ΔR were -43 ± 38 ^{14}C yr at 3885 cal yr BP and -183 ± 40 ^{14}C yr at 3862 cal yr BP. Hirabayashi et al. (2017a) reported similar variations at Ishigaki Island, varying from -136 ± 42 to 62 ± 50 ^{14}C yr in the late 1940s. Strong temporal and spatial fluctuations in ΔR values are observed in this region, which could be associated with ocean circulation, for example, as in the Bismarck Sea region (Petchey & Ulm, 2012).

4. Discussion

4.1. Regional short-term ΔR variability

ΔR values over the past 150 years from Lanyu Island is -5.3 ± 54 ^{14}C yr (Table 1), consistent with the modern values of -36.0 ^{14}C yr determined from Ishigaki Island and -36.6 ^{14}C yr from Kikai Island (Hirabayashi et al., 2017a), as well as the mean value of 4.5 ± 37 ^{14}C yr for Ishigaki Island in AD 1700-1900 (Araoka et al., 2010). The Lanyu's value is also identical to those of -19 yr and -13 yr from Palau and Guam, respectively (Andrews et al., 2016; Glynn et al., 2013). All of the above sites are located within the North Pacific gyre and gyre-fed currents, including the NEC and KC, which have ample opportunity at the surface for ^{14}C exchange with the atmosphere (Grottoli & Eakin, 2007; Mahadevan, 2001). ΔR is known to vary spatially and temporally due to the influence of regional hydrology, such as ocean circulation, upwelling, and river discharge. But the consistency of ΔR among sites suggests a common, predominant ^{14}C source in the western Pacific. As Lanyu is a small offshore island, terrestrial influences on the coral radiocarbon content can be ignored. Meanwhile, there is no major upwelling nearby. Therefore, the ΔR fluctuation on Lanyu probably reflects the ^{14}C content in seawater, carried by prevailing surface currents, i.e. the NEC and KC, in the neighborhoods of western Pacific.

Seasonal Δ^{14}C fluctuations have been reported in corals from Ishigaki Island, Palaui (Philippines), and southern Taiwan (Hirabayashi et al., 2017b; Mitsuguchi et al., 2004; Ramos et al., 2019). Mitsuguchi et al. (2004) and Ramos et al. (2019) both explained the relatively low Δ^{14}C in summer by the southwesterly monsoon-induced local upwelling. We averaged seasonal variations in our data by using a mixture of

coral fragments across several growth bands to measure ^{230}Th and ^{14}C ages. On interannual timescales, Ramos et al. (2019) pointed out that the Δ^{14}C difference between the northeastern Philippines and Guam mimics the meridional shift of the NEC bifurcation latitude (NBL), explained by the difference in transport velocities between the NEC and its branches. Moreover, larger ΔR values for the early 1900s from Palau, Guam and Okinawa have been also reported (Hirabayashi et al., 2017a; Southon et al., 2002; Yoneda et al., 2007). Hirabayashi et al. (2017a) attributed this so-called "early 20th-century positive-to-negative" shift in ΔR in the western Pacific to the influence of ENSO and PDO, because these two phenomena significantly affect the observed KC strength (Hu et al. 2015; Kashino et al., 2009; Qiu and Chen, 2010; Qiu, 2003), via a pressure difference from sea surface height changes (Ramos et al., 2019).

4.2. Centennial to millennial variability in ΔR values

A striking feature of the Lanyu results is the extremely low reservoir ages between 5950 and 5130 cal yr BP (Table 1). Large Holocene reservoir age shifts of this magnitude were reported in the South Pacific and South China Sea (SCS) (Burr et al., 2015; Hua et al., 2015; McGregor et al., 2008; Yu et al., 2010), albeit toward different directions. The regional sea level had reached the present level around 7 cal kyr BP (Liu et al., 2004), so the broad circulation pattern and geographical distribution then already resembled those of today (Kao et al., 2006). We thus excluded ocean circulation as the driver of this millennial change. Based on the coastal topography of Lanyu Island, possible change in coral habitat (Petchey and Clark, 2011), such as from lagoonal corals to open ocean equivalents, can also be ruled out. In fact, even if we conservatively consider a very low R values (<200 ^{14}C

250 years) for a lagoonal setting, the observed long-term trend of ΔR/R in the Holocene
251 will not change.
252 The skeletal $\Delta^{14}C$ value from Lanyu Island appeared to be closer to the IntCal09
253 curve (Fig. 2) during mid-Holocene. This implies a nearly pure atmospheric ^{14}C
254 signal and much intensified air-sea interactions, which could take place in the NEC,
255 KC, or both. For the NEC, it associates with the trade winds. The stronger the
256 easterly winds, the more intensified air-sea interaction and the more ^{14}C contents in
257 the surface NEC waters. For the KC, on top of the NEC inheritance, the East Asian
258 summer monsoon (EASM) also affects the KC strength, as well as the upwelling
259 activity and ^{14}C contents in the northern SCS. In fact, a stronger EASM (Dykoski et
260 al., 2005) associated with increased ΔR values in the northern SCS (Yu et al., 2010)
261 was observed for the mid-Holocene. As a result, strengthening of the trade winds in
262 the NEC and diminished EASM influence can both reduce the ΔR values in the
263 western Pacific.
264 On centennial timescales, a ~280 ^{14}C yr decrease in ΔR occurred during 3900–
265 3400 cal yr BP, and ΔR subsequently returned to a value of -34 ^{14}C yr in 3400–2700
266 cal yr BP (Fig. 3). Another similar ΔR fluctuation was observed in 950–150 cal yr BP
267 with a decrease of ~140 ^{14}C yr first and then an increase of ~230 ^{14}C yr (Fig. 3). The
268 amplitudes of the aforementioned fluctuations are conspicuous but are noticeably
269 smaller than those reported from south Peru (Fontugne et al., 2004) and Papua New
270 Guinea (McGregor et al., 2008), which were believed to sensitively reflect the
271 upwelling activity in the eastern Pacific. An intriguing observation here is that the
272 two centennial fluctuations are generally symmetric in time. This implies a fast-
273 restoring system most likely due to tightly coupled ocean and atmosphere, which was
274 mentioned in Burr et al. (2009).

4.3. Relationship between western Pacific ΔR and E–W Pacific gradient

Our results of reduced R and ΔR values from Lanyu Island (Fig. 2 & 3) suggest enhanced air-sea interactions during the mid-Holocene, and support the hypothesis of reduced ENSO frequency and a persistently La Niña-like state, which are inferred from both modeling and proxy-based paleoclimate studies (Clement et al., 2000; Koutavas et al., 2002; Liu et al., 2000; McGregor et al., 2008; Toth et al., 2015). The physical mechanism is detailed as bellow.

When the E–W Pacific gradient is larger, i.e. La Niña-like condition, the trade winds strengthen (Koutavas et al., 2002; Tian et al., 2018) alongside with enhanced air-sea interaction and long residence time at the surface, thus the NEC water reservoir age keeps decreasing as it flows westward. For the KC strength itself, modern observation suggests southward shift of the NEC bifurcation during La Niña periods, which associates with enforced Kuroshio transport east of Luzon (Masumoto and Yamagata, 1991; Tozuka et al., 2002) and diminished Kuroshio intrusion into the northern SCS (Qu et al., 2004). As a result, we speculates a relatively "poor-replenished SCS" under La Niña-like conditions during the mid-Holocene. An additional line of evidence is the SST offset between the western Pacific and northern SCS (Fig. 3).

The mechanism will evolve the other way around for a smaller E–W Pacific gradient, characterized with the El Niño regime. It causes a weaker KC east of Luzon, more Kuroshio water crossing the Luzon Strait (Chiang et al., 2010) and then an "open SCS". The seawater in the subtropical western Pacific, including Lanyu Island and the northern SCS, would consequently have a uniform $\Delta^{14}C$ or ΔR value. This prospect matches the modern Lanyu and northern SCS ΔR values, and is further

supported by the indistinguishable SST between these two areas (Fig. 3). To conclude, the ΔR from Lanyu Island reflects the ^{14}C signature in the KC, whereas the ^{14}C content in the northern SCS was influenced by other regional factors during the mid-Holocene, such as the EASM (Yu et al., 2010). Our hypothesis applicably explains the contrast pattern of ΔR values between Lanyu Island and the northern SCS over the past 6000 years. Our results also challenge the assumption of constant ΔR values and have important applications for palaeoclimatological, archaeological, and geohazard studies in the western Pacific regions in the future.

5. Conclusions

We presented radiocarbon marine reservoir ages (R) and regional marine reservoir corrections (ΔR) from the Lanyu Island, eastern Taiwan, over the past 6000 years using paired ^{14}C and ^{230}Th dating on 18 fossil corals. The extremely low reservoir ages and corrections in 6000–5100 cal yr BP indicate an enhanced E–W Pacific gradient and air-sea interactions. This condition favored a La Niña-like status in the Pacific basin, and likely produced an "isolated SCS" due to less Kuroshio penetration. The uniform ΔR value from Lanyu and northern SCS during late Holocene suggests an increased influence of the North Equatorial Current on the northern SCS.

Acknowledgments

We sincerely thank Dr. L.–H. Chung and Mr. Y.–L. Tsai for fieldwork assistance and Dr. X.F. Wang of the Earth observatory of Singapore, Nanyang Technological University, for providing constructive comments. This work was funded by the Ministry of Science and Technology (MOST), Taiwan, ROC (107–2116–M–002–

015–MY3 to H.–W.C., 104–2116–M–002–027–MY4 and 108–2116–M–002–016–MY2 to J.B.H.S.). U-Th dating was supported by grants from the Science Vanguard Research Program of the MOST (108-2119-M-002-012 to C.-C.S.) and the Higher Education Sprout Project of the Ministry of Education, Taiwan, ROC (108L901001 to C.-C.S.). The coral $R/\Delta R$ and $\Delta^{14}C$ data can be retrieved from the Dataset S1 and will be archived on the Mendeley Data (DOI is reserved but not active yet).

REFERENCES

Araoka, D., Inoue, M., Suzuki, A., Yokoyama, Y., Edwards, R. L., Cheng, H., et al. (2010). Historic 1771 Meiwa tsunami confirmed by high-resolution U/Th dating of massive Porites coral boulders at Ishigaki Island in the Ryukyus, Japan, *Geochemistry Geophysics Geosystems, 11*, Q06014, doi:10.1029/2009GC002893.

Andrews, A. H., Asami, R., Iryu, Y., Kobayashi, D. R., & Camacho, F. (2016). Bomb-produced radiocarbon in the western tropical Pacific Ocean: Guam coral reveals operation-specific signals from the Pacific Proving Grounds. *Journal of Geophysical Research: Oceans*, *121*, 6351–6366.

Broecker, W. S. (2014). Radiocarbon. In K. Turekian & H. Holland (Eds.), Treatise on geochemistry (2nd ed., Vol. 5, pp. 257–271). San Diego, La Jolla, CA: University of California, Elsevier Science.

Burr, G. S., Beck, J. W., Corrège, T., Cabioch, G., Taylor, F. W., & Donahue, D. J. (2009). Modern and Pleistocene reservoir ages inferred from South Pacific corals. *Radiocarbon, 51(1),* 319–335.

Burr, G. S., Haynes, C. V., Shen, C. C., Taylor, F., Chang, Y. W., Beck, J. W., et al. (2015). Temporal variations of radiocarbon reservoir ages in the South Pacific Ocean during the Holocene. *Radiocarbon*, *57*, 507–515. DOI: 10.2458/azu_rc.57.18460.

Chiang, H. W., Chen, Y. G., Fan, T. Y., & Shen, C. C. (2010). Change of the ENSO-related δ^{18}O–SST correlation from coral skeletons in northern South China Sea: A possible influence from the Kuroshio Current. *Journal of Asian Earth Sciences*, *39*, 684–691.

Clement, A. C., Seager, R., & Cane, M. A. (2000). Suppression of El Niño during the mid-Holocene by changes in the Earth's orbit. *Paleoceanography*, *15*, 731–737.

Cobb, K. M., Westphal, N., Sayani, H. R., Watson, J. T., Lorenzo, E. D., Cheng, H., et al. (2013). Highly variable El Niño-Southern Oscillation throughout the Holocene. *Science, 339*, 67–70. DOI:10.1126/science.1228246.

Druffel, E. R. M. (1997). Geochemistry of corals: proxies of past ocean chemistry, ocean circulation, and climate. *Proceedings of the National Academy of Sciences USA, 94(16)*, 8354–61.

Druffel, E. R. M. & Griffin, S. (1999). Variability of surface ocean radiocarbon and stable isotopes in the southwestern Pacific. *Journal of Geophysical Research, 104*, 607–613.

Dykoski, C. A., Edwards, R. L., Cheng, H., Yuan, D., Cai, Y., Zhang, M., et al. (2005). A high-resolution, absolute-dated Holocene and deglacial Asian monsoon record from Dongge Cave, China. *Earth Planetary Science Letters, 233*, 71–86.

Edwards, R. L., Chen, J. H., & Wasserburg, G. J. (1986/87). ^{238}U–^{234}U–^{230}Th–^{232}Th systematics and the precise measurement of time over the past 500,000 years. *Earth and Planetary Science Letters, 81*, 175–192.

Fontugne, M., Carré, M., Bentaleb, I., Julien, M., & Lavallée, D. (2004). Radiocarbon reservoir age variations in the South Peruvian upwelling during the Holocene. *Radiocarbon, 46*, 531–537.

Glynn, D., Druffel, E. R. M., Griffin, S., Dunbar, R., Osborne, M., & Sanchez-Cabeza, J. A. (2013). Early bomb radiocarbon detected in Palau archipelago corals. *Radiocarbon, 55*, 1659–1664. DOI:10.1017/S0033822200048578.

Grottoli, A. G., & Eakin, C. M. (2007). A review of modern coral $\delta^{18}O$ and $\Delta^{14}C$ proxy records. *Earth-Science Reviews, 81(1–2)*, 67–91. https://doi.org/10.1016/j.earscirev.2006.10.001

Hirabayashi, S., Yokoyama, Y., Suzuki, A., Miyairi, Y., & Aze, T. (2017a) Short-term fluctuations in regional radiocarbon reservoir age recorded in coral skeletons from the Ryukyu Islands in the north-western Pacific. *Journal of Quaternary Science*, *32*, 1–6. DOI:10.1002/jqs.2923.

Hirabayashi, S., Yokoyama, Y., Suzuki, A., Miyairi, Y., & Aze, T. (2017b) Multidecadal oceanographic changes in the western Pacific detected through high-resolution bomb-derived radiocarbon measurements on corals. *Geochemistry, Geophysics, Geosystems, 18*, 1608–1617. https://doi.org/10.1002/2017GC006854

Hsin, Y. C., Wu, C. R., & Shaw, P. T. (2008). Spatial and temporal variations of the Kuroshio east of Taiwan, 1982–2005, A numerical study. *Journal of Geophysical Research: Oceans, 113*, C04002. DOI:10.1029/2007JC004485.

Hu, D., Wu, L., Cai, W., Gupta, A. S., Ganachaud, A., Qiu, B., et al. (2015) Pacific western boundary currents and their roles in climate. *Nature, 522*, 299–308. DOI:10.1038/nature14504.

Hua, Q., Webb, G. E., Zhao, J.–X., Nothdurft, L. D., Lybolt, M., Price, G. J., et al. (2015). Large variations in the Holocene marine radiocarbon reservoir effect reflect ocean circulation and climatic changes. *Earth and Planetary Science Letters*, *422*, 33–44.

Inoue, S., Kayanne, H., Matta, N., Chen, W. S., & Ikeda, Y. (2011). Holocene uplifted coral reefs in Lanyu and Lutao Islands to the southeast of Taiwan. *Coral Reefs*, *30*, 581–592.

Kao, S. J., Wu, C. R., Hsin, Y. C., & Dai, M. H. (2006). Effects of sea level change on the upstream Kuroshio Current through the Okinawa Trough. *Geophysical Research Letters*, *33*, L16604. DOI:10.1029/2006GL026822.

Kashino, Y., España, N., Syamsudin, F., Richards, K. J., Jensen, T., Dutrieux, P., et al. (2009). Observations of the North Equatorial Current, Mindanao Current, and Kuroshio current system during the 2006/07 El Niño and 2007/08 La Niña. *Journal of Oceanography*, *65*, 325–333.

Kong, D., Zong, Y., Jia, G., Wei, G., Chen, M. T., & Liu, Z. (2014). The development of the late Holocene coastal cooling in the northern South China Sea. *Quaternary International*, *349*, 300–307.

Koutavas, A., Lynch–Stieglitz, J., Marchitto, Jr. T. M., & Sachs, J. P. (2002) El Niño-like pattern in Ice Age tropical Pacific sea surface temperature. *Science*, *297*, 226–230.

Lee, T. N., Johns, W. E., Liu, C. T., Zhang, D., Zantopp, R., & Yang, Y. (2001). Mean transport and seasonal cycle of the Kuroshio east of Taiwan with comparison to the Florida Current. *Journal of Geophysical Research: Oceans*, *106*, 22143–22158. DOI:10.1029/2000JC000535.

Liang, W. D., Tang, T. Y., Yang, Y. J., Ko, M. T., & Chuang, W. S. (2003). Upper-ocean currents around Taiwan. *Deep Sea Research Part II: Topical Studies in Oceanography*, *50*, 1085–1105. DOI:10.1016/S0967-0645(03)00011-0.

Liu, J. P., Milliman, J. D., Gao, S., & Cheng, P. (2004). Holocene development of the Yellow River's subaqueous delta, North Yellow Sea. *Marine Geology*, *209*, 45–67. DOI:10.1016/j.margeo.2004.06.009.

Liu, Z., Kutzbach, J., & Wu, L. (2000). Modeling climate shift of El Niño variability in the Holocene. *Geophysical Research Letters*, *27*, 2265–2268.

Lo, L., Lai, Y. H., Wei, K. Y., Lin, Y. S., Mii, H. S., & Shen, C. C. (2013). Persistent sea surface temperature and declined sea surface salinity in the northwestern

tropical Pacific over the past 7500 years. *Journal of Asian Earth Sciences*, *66*, 234–239.

Mahadevan, A. (2001). An analysis of bomb radiocarbon trends in the Pacific. *Marine Chemistry*, *73(3-4)*, 273–290. https://doi.org/10.1016/S0304-4203(00)00113-4

Masumoto, Y., & Yamagata, T. (1991). Response of the western tropical Pacific to the Asian winter monsoon: the generation of the Mindanao Dome. *Journal of Physical Oceanography*, *21*, 1386–1398.

McGregor, H. V., & Gagan, M. K. (2004). Western Pacific coral $\delta^{18}O$ records of anomalous Holocene variability in the El Niño–Southern Oscillation. *Geophysical Research Letters*, *31*, L11204. DOI:10.1029/2004GL019972.

McGregor, H. V., Gagan, M. K., McCulloch, M. T., Hodge, E., & Mortimer, G. (2008). Mid-Holocene variability in the marine ^{14}C reservoir age for northern coastal Papua New Guinea. *Quaternary Geochronology*, *3*, 213–225. DOI:10.1016/j.quageo.2007.11.002.

Mitsuguchi, T., Kitagawa, H., Matsumoto, E., Shibata, Y., Yoneda, M., Kobayashi, T., et al. (2004). High-resolution ^{14}C analyses of annually banded coral skeletons from Ishigaki Island, Japan: implications for oceanography. *Nuclear Instruments and Methods in Physics Research Section B: Beam Interactions with Materials and Atoms*, *223–224*, 455–459. DOI:10.1016/j.nimb.2004.04.086.

Moy, C. M., Seltzer, G. O., Rodbell, D. T., & Anderson, D. M. (2002). Variability of El Niño/Southern Oscillation activity at millennial timescales during the Holocene epoch. *Nature*, *420*, 162–165. DOI:10.1038/nature01194.

Moyer, R. P., & Grottoli, A. G. (2011). Coral skeletal carbon isotopes ($\delta^{13}C$ and $\Delta^{14}C$) record the delivery of terrestrial carbon to the coastal waters of Puerto Rico. *Coral Reefs*, *30*, 791–802.

Nozaki, Y., Rye, D. M., Turekian, K. K., & Dodge, R. E. (1978). A 200 year record of ^{13}C and ^{14}C variations in a Bermuda coral. *Geophysical Research Letters*, *5*, 825–828.

Ota, Y., Shyu, J. B. H., Wang, C. C., Lee, H. C., Chung, L. H., & Shen, C. C. (2015). Coral boulders along the coast of the Lanyu Island, offshore southeastern Taiwan, as potential paleotsunami records. *Journal of Asian Earth Sciences*, *114*, 588–600. DOI:10.1016/j.jseaes.2015.08.001.

Petchey, F., & Clark, G. (2011). Tongatapu hardwater: Investigation into the ^{14}C marine reservoir offset in lagoon, reef and open ocean environments of a limestone island. *Quaternary Geochronology*, *6*, 539–549.

Petchey, F., & Ulm, S. (2012). Marine reservoir variation in the Bismarck Region: an evaluation of spatial and temporal change in ΔR and R over the last 3000 years. *Radiocarbon*, *54*, 45–58.

Qiu, B. (2003). Kuroshio Extension variability and forcing of the Pacific decadal oscillations: Responses and potential feedback. *Journal of Physical Oceanography*, *33*, 2465–2482.

Qiu, B., & Chen, S. (2010). Interannual-to-decadal variability in the bifurcation of the North Equatorial Current off the Philippines. *Journal of Physical Oceanography*, *40(11)*, 2525–2538. https://doi.org/10.1175/2010JPO4462.1

Qu, T., Kim, Y. Y., & Yaremchuk, M. (2004). Can Luzon Strait transport play a role in conveying the impact of ENSO to the South China Sea? *Journal of Climate*, *17(18)*, 3644–3657. https://doi.org/10.1175/1520-0442(2004)017

Qu, T., & Lukas, R. (2003). The bifurcation of the North Equatorial Current in the Pacific. *Journal of Physical Oceanography*, *33*, 5–18.

Ramos, R. D., Goodkin, N. F., Druffel, E. R. M., Fan, T. Y., & Siringan, F. P. (2019). Interannual coral $\Delta^{14}C$ records of surface water exchange across the Luzon Strait. *Journal of Geophysical Research: Oceans*, *124*. https://doi.org/ 10.1029/2018JC014735

Reimer, P. J. and 27 others (2009) IntCal09 and Marine09 radiocarbon age calibration curves, 0-50,000 years cal BP. *Radiocarbon*, *51*, 1111–1150.

Shen, C.-C., Cheng H., Edwards R. L., Moran S. B., Edmonds H. N., Hoff J. A., et al. (2003) Measurement of attogram quantities of ^{231}Pa in dissolved and particulate fractions of seawater by isotope dilution thermal ionization mass spectroscopy. *Analytical Chemistry*, *75*, 1075-1079.

Shen, C. C., Wu, C. C., Cheng, H., Edwards, R. L., Hsieh, Y. T., Gallet, S., et al. (2012). High-precision and high-resolution carbonate ^{230}Th dating by MC-ICP-MS with SEM protocols. *Geochimica et Cosmochimica Acta*, *99*, 71–86.

Southon, J. R., Kashgarian, M., Fontugne, M., Metivier, B., & Yim, W. W.-S. (2002). Marine reservoir corrections for the Indian Ocean and southeast Asia. *Radiocarbon*, *44*, 167–180.

Stein, M., Wasserburg, G. J., Aharon, P., Chen, H., Zhu, Z. R., Bloom, A., et al. (1993). TIMS U-series dating and stable isotopes of the last interglacial event in Papua New Guinea. *Geochimica et Cosmochimica Acta, 57*, 2541–2554.

Stirling, C. H., Esat, T. M., McCulloch, M. T., & Lambeck, K. (1995). High-precision U-series dating of corals from Western Australia and implications for the timing and duration of the Last Interglacial. *Earth and Planetary Science Letters*, *135*, 115–130.

Stuiver, M., Pearson, G. W., & Braziunas, T. (1986). Radiocarbon age calibration of marine samples back to 9000 cal yr BP. *Radiocarbon*, *28*, 980–1021.

Stuiver, M., & Polach, H. (1977). Discussion: reporting of ^{14}C data. *Radiocarbon*, *19(3)*, 355–63.

Tian, Z., Li, T., Jiang, D., & Chen, L. (2018). Strengthening and Westward Shift of the Tropical Pacific Walker Circulation during the Mid-Holocene: PMIP Simulation Results. *Journal of Climate*, *31*, 2283–2296.

Toth, L. T., Aronson, R.B., Cheng, H., & Edwards, R. L. (2015). Holocene variability in the intensity of wind-gap upwelling in the tropical eastern Pacific, *Paleoceanography*, *30*, 1113–1131, doi:10.1002/2015PA002794.

Tozuka, T., Kagimoto, T., Masumoto, Y., & Yamagata, T. (2002). Simulated multiscale variations in the western tropical Pacific: The Mindanao Dome revisited. *Journal of Physical Oceanography*, *32*, 1338–1359.

Tudhope, A. W., Chilcott, C. P., McCulloch, M. T., Cook, E. R., Chappell, J., Ellam, R. M., et al. (2001). Variability in the El Niño–Southern Oscillation through a glacial–interglacial cycle. *Science*, *291*, 1511–1517.

Yaremchuk, M., & Qu, T. D. (2004). Seasonal variability of the large-scale currents near the coast of the Philippines. *Journal of Physical Oceanography*, *34*, 844–855. DOI:10.1175/1520-0485(2004)034<0844:SVOTLC>2.0.CO;2.

Yoneda, M., Uno, H., Shibata, Y., Suzuki, R., Kumamoto, Y., Yoshida, K., et al. (2007). Radiocarbon marine reservoir ages in the western Pacific estimated by pre-bomb molluscan shells. *Nuclear Instruments and Methods in Physics Research Section B: Beam Interactions with Materials and Atoms*, *259*, 432–437. DOI:10.1016/j.nimb.2007.01.184.

Yu, K. F., Hua, Q., Zhao, J. X., Fink, D., & Barbetti, M. (2010). Holocene marine ^{14}C reservoir age variability: Evidence from ^{230}Th-dated corals in the South China Sea. *Paleoceanography*, *25*, PA3205. DOI:10.1029/2009PA001831.

Zaunbrecher, L. K., Cobb, K. M., Beck, J. W., Charles, C. D., Druffel, E. R. M., Fairbanks, R. G., et al. (2010). Coral records of central tropical Pacific radiocarbon variability during the last millennium. *Paleoceanography*, *25*, PA4212. DOI:10.1029/2009PA001788.

Zhang, Z., Leduc, G., & Sachs, J. P. (2014). El Niño evolution during the Holocene revealed by a biomarker rain gauge in the Galápagos Islands. *Earth and Planetary Science Letters*, *404*, 420–434. http://dx.doi.org/10.1016/j.epsl.2014.07.013

Figure Captions

Figure 1. (a) Geographical map of the western Pacific, with the route of the North Equatorial Current (NEC) and the Kuroshio Current (KC) shown as blue shadowed arrows. In the present day, the main stream of the KC flows northward off the eastern coast of Taiwan, but a westward branch may seasonally penetrate into the northern South China Sea. The locations of other ΔR records are also marked as white circles, with SST and monsoon records mentioned in the text as white triangles. (b) Geomorphic map of Lanyu Island with the six sampling sites along its northern coast. Modified from Ota et al. (2015). (KE, Kuroshio Extension; MC, Mindanao Current)

Figure 2. Comparison of $\Delta^{14}C$ of Lanyu corals with the IntCal09 (dark gray) and Marine09 (light gray) curves. Insert is the ΔR data of Lanyu and Ryukyu Islands (Yoneda et al., 2007; Hirabayashi et al., 2017a) in the past 150 years. Age axis is based on U–Th and band-counting results for the Lanyu and Ryukyu corals, respectively. The hollow circles indicate the 5 replicates analyzed in XAAMS.

Figure 3. Comparison of the (c) Lanyu ΔR results (solid circles) with (b) SCS data (green hollow circles, Yu et al., 2010). The $\delta^{18}O$ record from (a) Dongge cave, China, is shown in the upper panel as the proxy of Asian summer monsoon (Dykoski et al., 2005). Foraminifera Mg/Ca ratio-inferred SST are from two cores: (d) OR1715-21 (purple, Lo et al., 2013) and (e) NS02G (light green, Kong et al., 2014). (f) Gray line shows the ENSO frequency recorded in sediments from southern Ecuador (Moy et al., 2002). Red circles: radiocarbon dating analyzed by Beta Analytic, Inc.; blue circles: radiocarbon dating analyzed in XAAMS.

Figure.

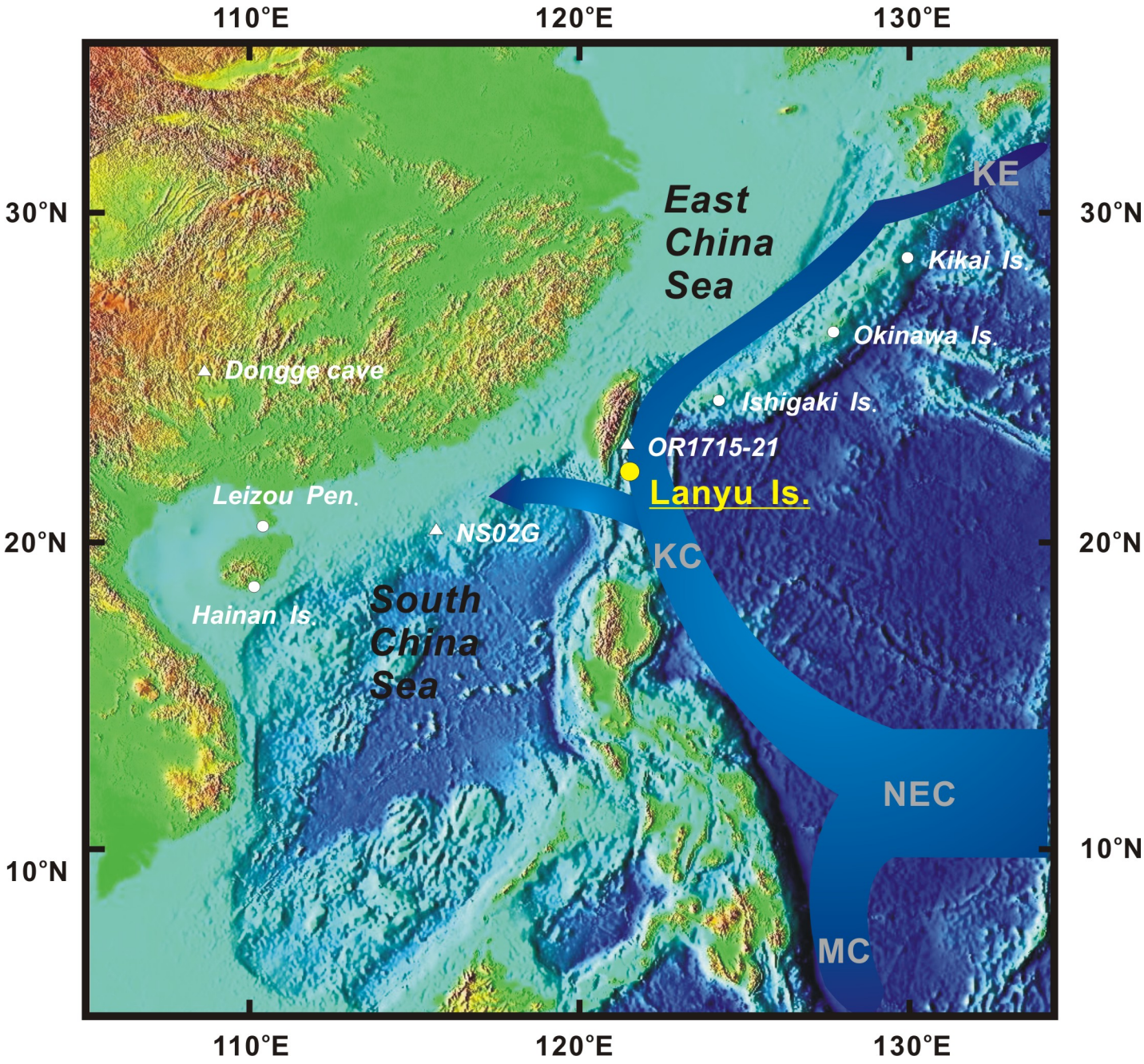
110°E
120°E
130°E
30°N
20°N
10°N
East China Sea
South China Sea
KE
KC
NEC
MC
Kikai Is.
Okinawa Is.
Ishigaki Is.
Dongge cave
OR1715-21
Lanyu Is.
Leizou Pen.
NS02G
Hainan Is.

Figure 1a

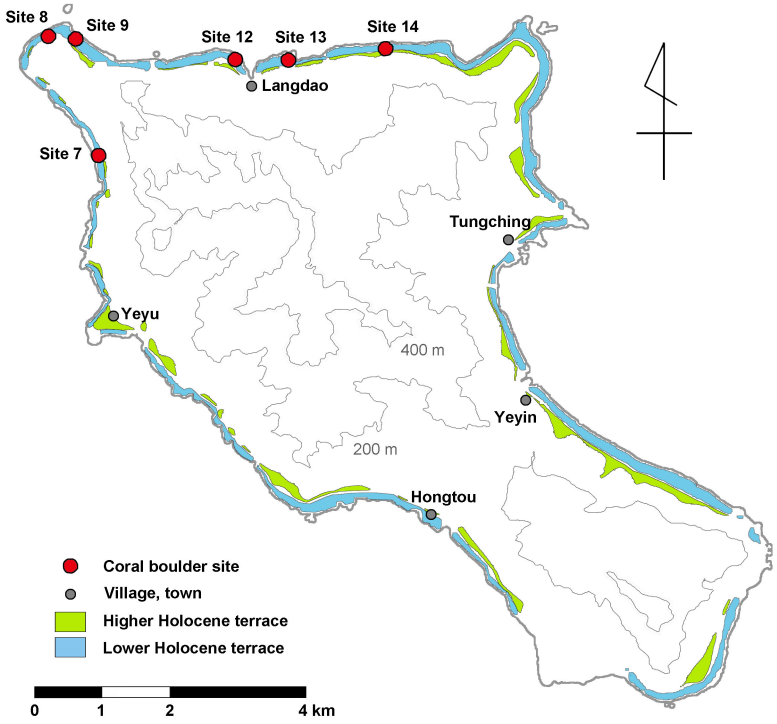
Site 8
Site 9
Site 12
Site 13
Site 14
Langdao
Site 7
Tungching
Yeyu
400 m
Yeyin
200 m
Hongtou
Coral boulder site
Village, town
Higher Holocene terrace
Lower Holocene terrace
0
1
2
4 km

Figure 1b

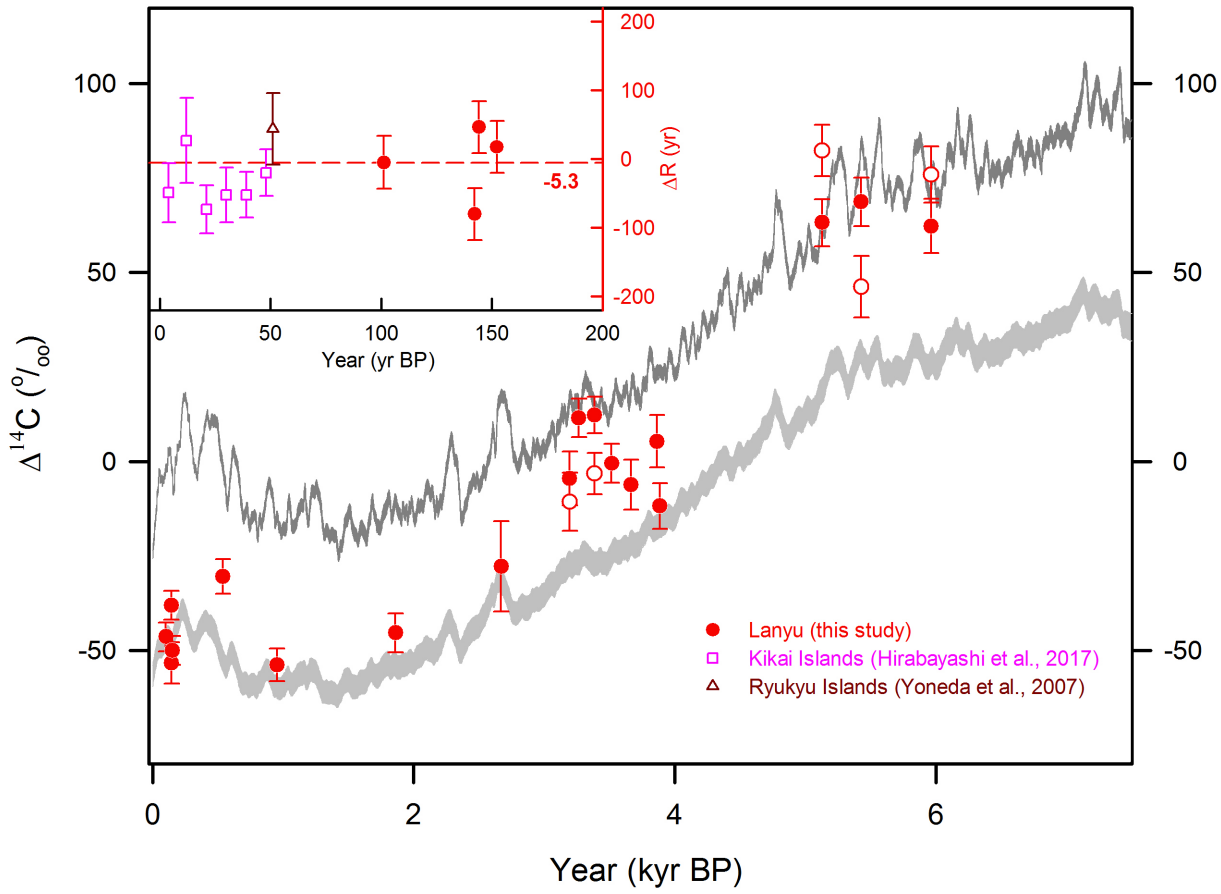
100
50
0
-50
$\Delta^{14}C$ ($^{o}/_{oo}$)
0
2
4
6
Year (kyr BP)
200
100
0
-100
-200
ΔR (yr)
-5.3
0
50
100
150
200
Year (yr BP)
Lanyu (this study)
Kikai Islands (Hirabayashi et al., 2017)
Ryukyu Islands (Yoneda et al., 2007)

Figure 2

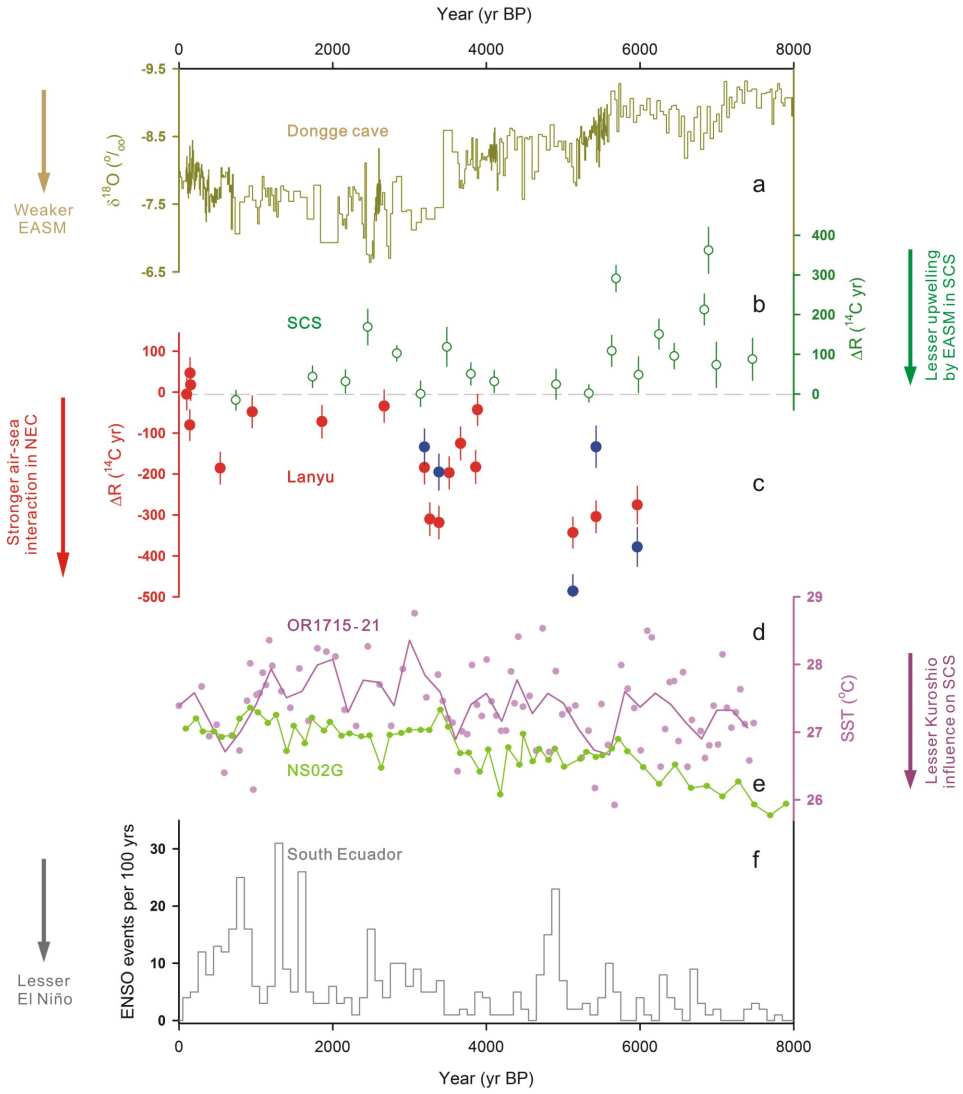
Year (yr BP)
0
2000
4000
6000
8000
Dongge cave
δ18O (‰)
-9.5
-8.5
-7.5
-6.5
a
Weaker EASM
400
300
200
100
0
ΔR (14C yr)
b
SCS
Lesser upwelling by EASM in SCS
100
0
-100
-200
-300
-400
-500
ΔR (14C yr)
Lanyu
c
Stronger air-sea interaction in NEC
OR1715-21
d
29
28
27
26
SST (°C)
Lesser Kuroshio influence on SCS
NS02G
e
South Ecuador
f
ENSO events per 100 yrs
30
20
10
0
Lesser El Niño
Year (yr BP)

Figure 3

Table 1. Results of marine reservoir age and corrections (R, ΔR) for Lanyu Island

Sample	Conventional ^{14}C age (^{14}C yr BP)	U-Th age (yr BP)[a]	Atmosphere modeled age (IntCal09, ^{14}C yr BP)[b]	Marine modeled age (Marine09, ^{14}C yr BP)[b]	R (^{14}C yr)[c,d]	ΔR (^{14}C yr)[c,d]	Δ^{14}C (‰)[e]
12-1	480 ± 30	101.2 ± 2.1	113.2 ± 9.0	485 ± 24	367 ± 31	-5 ± 38	-46 ± 3
8-1-5	450 ± 30	142.2 ± 1.9	140.4 ± 8.0	530 ± 23	310 ± 31	-80 ± 38	-38 ± 3
8-1-2	580 ± 30	144 ± 17	148.8 ± 8.0	533 ± 23	431 ± 31	47 ± 38	-53 ± 7
8-1-1	560 ± 30	152.2 ± 2.2	186.6 ± 8.0	542 ± 23	373 ± 31	18 ± 38	-50 ± 3
9-2	770 ± 30	536.7 ± 8.5	533 ± 12	956 ± 25	237 ± 32	-186 ± 39	-30 ± 1
13-1	1370 ± 30	952.5 ± 7.2	1042 ± 12	1418 ± 25	328 ± 32	-48 ± 39	-54 ± 1
13-2	2180 ± 30	1860 ± 13	1890 ± 14	2252 ± 26	290 ± 33	-72 ± 40	-45.3 ± 0.7
8-3	2820 ± 30	2670 ± 71	2456 ± 14	2854 ± 26	364 ± 33	-34 ± 40	-27.7 ± 0.8
13-3	3140 ± 30	3194 ± 28	2971 ± 16	3324 ± 27	169 ± 34	-184 ± 40	-4.5 ± 0.1
	3190[f] ± 35				*219 ± 38*	*-134 ± 44*	*-10.7 ± 0.2*
12-1-4	3080 ± 30	3264 ± 11	3051 ± 16	3390 ± 27	29 ± 34	-310 ± 40	11.5 ± 0.1
9-3	3190 ± 30	3383.4 ± 8.8	3167 ± 15	3509 ± 26	23 ± 34	-319 ± 40	12.2 ± 0.1
	3313[f] ± 35				*146 ± 38*	*-195 ± 44*	*-3.20 ± 0.04*
9-4	3420 ± 30	3515 ± 11	3307 ± 14	3617 ± 26	113 ± 33	-197 ± 40	-0.520 ± 0.005
9-5	3610 ± 30	3664 ± 24	3411 ± 16	3735 ± 27	199 ± 34	-125 ± 40	-6.2 ± 0.1
8-2	3710 ± 30	3862 ± 26	3566 ± 16	3893 ± 27	144 ± 34	-183 ± 40	5.3 ± 0.1
14-2	3870 ± 30	3885 ± 20	3582.0 ± 9.0	3913 ± 24	288 ± 31	-43 ± 38	-11.8 ± 0.1
7-2	4490 ± 30	5127 ± 17	4500 ± 14	4833 ± 23	-10 ± 33	-343 ± 38	63.2 ± 0.5
	4347[f] ± 34				*-153 ± 36*	*-486 ± 41*	*82.3 ± 0.7*
9-1	4740 ± 30	5427 ± 19	4627 ± 12	5044 ± 25	113 ± 32	-304 ± 39	68.7 ± 0.5
	4911[f] ± 45				*284 ± 46*	*-134 ± 51*	*46.2 ± 0.4*
7-1	5310 ± 40	5964 ± 15	5234 ± 15	5586 ± 23	76 ± 43	-276 ± 46	62.3 ± 0.5
	5207[f] ± 42				*-26 ± 44*	*-378 ± 48*	*75.9 ± 0.6*

[a] Calendar years before AD 1950.

[b] U-Th ages were converted to atmosphere (marine) model ages (1σ) using Intcal09 (Marine09) data (Reimer et al., 2009).

[c] The marine model age error (1σ) is the mean of the span of the mean and oldest/youngest ^{14}C ages.

[d] R and ΔR were calculated using Eq. (1) and (2), respectively. The 1σ error is $(1\sigma^2_{\text{conventional }^{14}\text{C age}}+1\sigma^2_{\text{model age}})^{1/2}$.

[e] The 1σ error is $(1\sigma^2_{\text{U-Th age}}+1\sigma^2_{\text{model age}})^{1/2}$.

[f] ^{14}C ages done in Xi'an accelerator mass spectrometry center.